Spectrochimica Acta Part A: Molecular and Biomolecular Spectroscopy 206 (2019) 437–447

Contents lists available at ScienceDirect

Spectrochimica Acta Part A: Molecular and Biomolecular Spectroscopy

journal homepage: www.elsevier.com/locate/saa

Inhibition of α-amylase by flavonoids: Structure activity relationship (SAR)

Martinez-Gonzalez A.I. [a], Díaz-Sánchez Á.G. [a], de la Rosa L.A. [a], Bustos-Jaimes I. [b], Alvarez-Parrilla E. [a,*]

[a] Departamento de Ciencias Químico Biológicas, Instituto de Ciencias Biomédicas, Universidad Autónoma de Ciudad Juárez, Ciudad Juárez 32310, Mexico
[b] Departamento de Bioquímica, Facultad de Medicina, Universidad Nacional Autónoma de México, México D.F. 04510, Mexico

ARTICLE INFO

Article history:
Received 15 May 2018
Received in revised form 14 August 2018
Accepted 27 August 2018
Available online 28 August 2018

Keywords:
Flavonoids
α-Amylase
Interactions
Inhibition
Structure
Luteolin

ABSTRACT

Flavonoids are recognized to regulate animals' food digestion processes trough interaction with digestive enzymes. The binding capacity of hesperetin (HES), luteolin (LUT), quercetin (QUE), catechin (CAT) and rutin (RUT) with pancreatic α-amylase were evaluated, using UV–Vis spectroscopy, fluorescence and molecular docking. Using *p*-nitrophenyl-α-D-maltopentoside (*p*NPG5) as substrate analog, LUT showed the best inhibitory capacity, even better than that of the positive control, acarbose (ACA). A mixed-type inhibition was observed for HES, LUT and QUE, a competitive-type for ACA, while no inhibition was observed with CAT and RUT. In agreement with kinetic results, α-amylase presented a higher affinity for LUT, when analyzed by fluorescence quenching. The binding of flavonoids to amylase followed a static mechanism, where the binding of one flavonoid per enzyme molecule was observed. Docking analysis showed that flavonoids bound near to enzyme active site, while ACA bound in another site behind the catalytic triad. Extrinsic fluorescence analysis, together with docking analysis pointed out that hydrophobic interactions regulated the flavonoid-α-amylase interactions. The present study provides evidence to understand the relationship of flavonoids structure with their inhibition mechanism.

1. Introduction

Structure-activity relationship (SAR) is the association between the structure of bioactive compounds to their biological/chemical effect. SAR has been used to explain the effect of structural features of molecules on their activity, and is considered a key tool for drug discovery [1]. SAR analysis with polyphenolic compounds (PC) has been used to evaluate their relationship with antioxidant activities [2,3]. In the case of flavonoids SAR has been related to changes on their structures, for example, the hydroxyl (—OH) groups at C-3, C-7 and C-4′, the presence or absence of a carbonyl group in ring C, which regulates the flexibility or the molecule, among other properties [3]. Flavonoids can be divided into different subgroups depending on the substitution in the heterocyclic ring (ring C) [4]. Flavanones (such as hesperetin, herein named as HES), flavones (luteolin, LUT), flavonols (quercetin, QUE), and flavanols (catechin, CAT) are some of the most relevant subgroups (Fig. 1). Flavonoids commonly are present as glycosylated forms, by joining to a sugar moiety, for example rutin (RUT).

Other beneficial effect of PC, besides the antioxidant ability, is related to their inhibitory activity against digestive enzymes [5,6]. SAR studies help to elucidate the process behind the interaction and the subsequent inhibition of these enzymes. Digestive enzymes such as pancreatic α-amylase have been inhibited in presence of PC, and plant phenolic extracts [7–9]. α-Amylase is a drug target to control the amount of sugar absorbed during feeding and one of the therapeutic treatments for diabetes disease include the uptake of the α-amylase inhibitor acarbose (ACA). However, the use of ACA presents several side effects like gastrointestinal disturbances [10]. Finding alternative innocuous inhibitors for α-amylase is relevant to couple with post-prandial hyperglycemia [11,12]. One of such inhibitors could be natural compounds as flavonoids that could be naturally ingested in the diet [13].

Even though, a mixed-type inhibition has been reported for most PC, the interaction mechanism remains unclear. Flavonoids exhibit higher inhibitory capacity, compared to other PC [14,15], but as in the case of other PC, neither the interaction mode nor the binding site with the enzyme have been fully described. SAR analysis for α-amylase-flavonoids interactions suggested that the number and position of hydroxyl groups in the flavonoid structure regulates their inhibitory activities [16]. However, more studies are required to elucidate the possible SAR mechanism

Abbreviations: SAR, structure-activity relationship; HES, hesperetin; LUT, luteolin; QUE, quercetin; CAT, catechin; RUT, rutin; ACA, acarbose; PC, polyphenolic compounds; *p*NPG5, *p*-nitrophenyl-α-D-maltopentoside.

* Corresponding author.
E-mail addresses: angel.diaz@uacj.mx (Á.G. Díaz-Sánchez), ldelaros@uacj.mx (L.A. de la Rosa), ismaelb@unam.mx (I. Bustos-Jaimes), ealvarez@uacj.mx (E. Alvarez-Parrilla).

https://doi.org/10.1016/j.saa.2018.08.057
1386-1425/

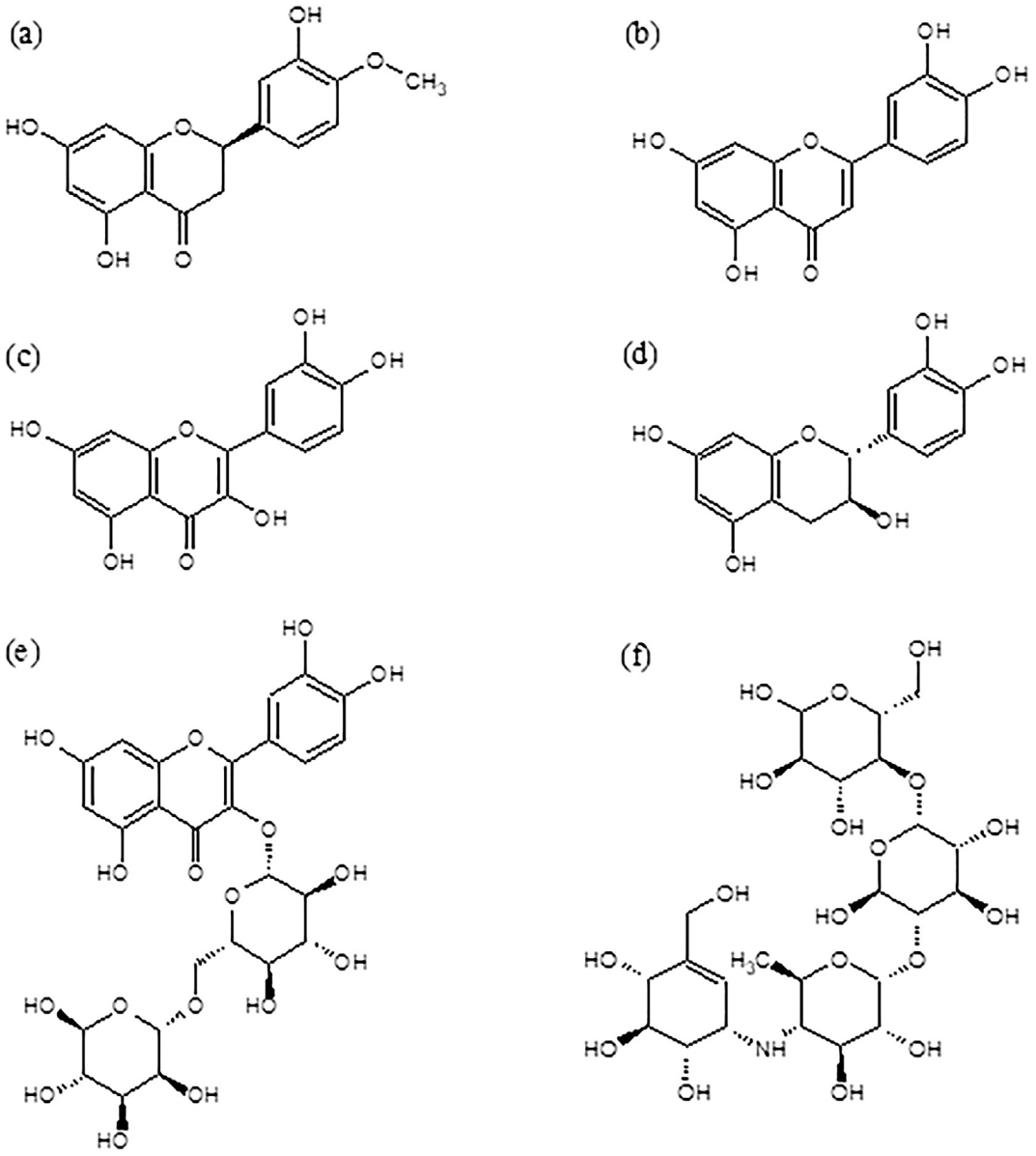

Fig. 1. Chemical structures of analyzed flavonoids, hesperetin (a, HES), luteolin (b, LUT), quercetin (c, QUE), catechin (d, CAT), and rutin (e, RUT); and acarbose (f, ACA).

involved in these α-amylase-flavonoid complexes, through UV–Vis spectroscopy, (intrinsic and extrinsic) fluorescence and molecular docking. For this reason, in the present study, the interactions of five typical flavonoids with α-amylase was carried out, to give a detailed description of the best inhibitor characteristics and its binding site on enzyme, for further comprehension of α-amylase-flavonoids interaction.

2. Experimental

2.1. Materials

Pancreatic α-amylase type I-A was purchased from Sigma-Aldrich Co. (Mexico). According to SDS-PAGE analysis, the enzyme purity was calculated to be 95%, and no further purification step was necessary (data not shown). Flavonoids (HES, LUT, QUE, CAT and RUT), ACA, 4-(2-hydroxyethyl) piperazine-1-ethanesulfonic (HEPES) sodium salt, *p*-nitrophenyl-α-D-maltopentoside (*p*NPG5), and 8-anilino-1-naphtalenesulfonic acid (ANS) were also from Sigma-Aldrich Co. Methanol was purchased from J.T. Baker (USA). All chemicals were of analytical-reagent grade.

2.2. Pancreatic α-Amylase Activity Assay

The enzymatic activity was assayed according to Gonçalves, Mateus and Freitas [17] with some modifications. Pancreatic α-amylase and substrate, *p*NPG5, were dissolved in HEPES buffer (50 mM, pH 7.0). Final pancreatic α-amylase concentration was 1 μM. *p*NPG5 final concentrations were 0.3–2.7 mM. Flavonoids were dissolved in methanol and ACA in distilled water.

The control assay contained HEPES buffer, distilled water, pancreatic α-amylase solution, and substrate solution. For the inhibition studies, the corresponding volume of flavonoid for each final concentration, was subtracted from the volume of distilled water. The substrate was added to start the reaction, then *p*-nitrophenol released by pancreatic α-amylase activity over the substrate was measured at 400 nm during 120 min at 37 °C in a UV/Vis microplate spectrophotometer (Bio-Rad xMark™, USA). All samples were assayed by triplicate.

The inhibition percentage (Eq. (1)) was calculated as Dalar and Konczak [18] from endpoint registration.

$$\text{Inhibition percentage} = \frac{(A_{cb} - A_c) - (A_{sb} - A_s)}{A_{cb} - A_c} \cdot 100 \quad (1)$$

where A_{cb} is the absorbance of the control blank, A_c is the absorbance of the control, A_{sb} is the absorbance of the sample blank, and A_s is the absorbance of the sample. Both blanks were prepared by replacing the pancreatic α-amylase solution and the *p*NPG5 solution, respectively. IC_{50} was calculated from an inhibitor concentration *versus* inhibition percentage plot.

The Michaelis-Menten kinetic model was employed to analyze the effect of flavonoids on *p*NPG5 hydrolysis. The apparent catalytic parameters, maximal reaction rate (V_{max}) and Michaelis-Menten constant (K_M) were calculated in the absence and presence of the flavonoids. K_i values of flavonoids and ACA were determined by calculating V_{max} and K_M by both non-linear (Michaelis-Menten) and linear (Lineweaver-Burk) analyses as in Heredia et al. [19] and Martinez-Gonzalez et al. [6]. The non-linear analysis was performed at Sigma Plot v. 12.0 using Eq. (2). Lineweaver-Burk analysis was performed with Eq. (3).

$$v_0 = \frac{V_{max} \cdot \left([S]^h\right)}{K_M + \left([S]^h\right)} \quad (2)$$

$$\frac{1}{v_0} = \frac{1}{V_{max}} + \frac{K_M}{V_{max} \cdot \left([S]^h\right)} \quad (3)$$

where *h* was the Hill coefficient value determined by the non-linear curve fitting of kinetic time course in absence and presence of the flavonoids.

K_i and K_i' (dissociation constant for free enzyme and enzyme-substrate complex, respectively) values for a mixed-type inhibition were obtained for mixed-type inhibition by fitting the experimental data to Eqs. (4) and (5) [20].

$$\frac{K_M'}{V_{max}'} = \frac{K_M \cdot \left(1 + \frac{[I]}{K_i}\right)}{V_{max}} \quad (4)$$

$$V_{max}' = \frac{V_{max}}{\left(1 + \frac{[I]}{K_i'}\right)} \quad (5)$$

K_i for ACA was determined using Eq. (6) [20] considering a competitive-type inhibition mechanism.

$$K_M' = K_M \cdot \left(1 + \frac{[I]}{K_i}\right) \quad (6)$$

where [I], K_M' and V_{max}' corresponded to the inhibitor concentration, and the Michaelis-Menten constant and the maximal reaction rate values in presence of inhibitor, respectively.

2.3. Pancreatic α-Amylase-flavonoid Interaction Measured by the Intrinsic Fluorescence Spectra

The quenching effect of the ligands (HES, LUT, QUE, CAT, RUT, and ACA) on pancreatic α-amylase fluorescence intensity was assayed as described in the literature with some modifications [21,22]. The binding between pancreatic α-amylase and the analyzed compounds was registered after apparent equilibrium. The intrinsic tryptophan (Trp) fluorescence intensity changes were measured on a spectrofluorometer microplate reader (FLUOstar Omega™, USA). The sample of the pancreatic α-amylase solution (1 μM, HEPES buffer pH 7.0) and distilled water, in the absence or presence of different concentrations (3–100 μM) of flavonoids and ACA, was incubated at 37 °C for 1 h, and then the sample was excited at 290 nm and the fluorescence emission was recorded at 340 nm. A control experiment with solvent at same volumes as in the ligand additions was carried on, and fluorescence intensities were corrected for inner filter effects. The flavonoids did not exhibit FRET at that excitation wavelength. Fluorescence intensity changes were plotted against the flavonoid concentrations and fitted to Eq. 7.

$$\Delta FI = \frac{B_{max} \cdot [I]}{K_D + [I]} \quad (7)$$

where ΔFI is the change in fluorescence intensity at 340 nm; B_{max} is the maximum Δ*FI*; K_D corresponds to the dissociation constant; and *I* is the inhibitor concentration.

The fluorescence quenching parameters were calculated from the linear Stern-Volmer Eq. (8) [23].

$$\frac{F_0}{F} = 1 + k_q \tau_0 [Q] = 1 + K_{sv}[Q] \quad (8)$$

where F_0 and *F* are the fluorescence intensities in the absence and presence of the quencher (herein refers to flavonoids), respectively. k_q, τ_0, and K_{sv} are the bimolecular quenching constant, the lifetime of the fluorescence in the absence of the quencher, and the Stern-Volmer quenching constant, respectively whereas [Q] is the concentration of the quencher. τ_0 value is equal to 2.97 ns according to Prendergast, Lu and Callahan [24].

Eq. (9) is a modification of Stern-Volmer equation (Eq. (8)) used to estimate the apparent values of the associative binding constant (K_a) of the enzyme-flavonoid complex, and the number of binding sites per protein (*n*) [23].

$$\log \frac{F_0 - F}{F} = \log K_a + n \log[Q] \quad (9)$$

2.4. Binding of Flavonoids to Pancreatic α-Amylase by the Extrinsic Fluorescence of ANS

To further study the binding between pancreatic α-amylase and flavonoids, the surface hydrophobicity of pancreatic α-amylase was measured using the extrinsic fluorescence probe ANS [25,26]. Fluorescence emission measurements were performed in a Shimadzu RF-5301 spectrofluorometer (USA). α-Amylase (1 μM) was incubated with ANS (150 μM) at 37 °C for 15 min. Flavonoids or ACA (up to 149 μM) were titrated (15 injections) into the spectrofluorometer cell containing enzyme and ANS. The excitation wavelength was set at 380 nm at 37 °C. Fluorescence emission spectra was recorded from 400 to 700 nm (monitored at 519 nm) from samples loaded into a 1 cm path-length quartz cuvette. Fluorescence intensities were corrected for volume changes and inner filter effects.

2.5. Molecular Docking

Was performed similar as in Martinez-Gonzalez, Alvarez-Parrilla, Díaz-Sánchez, de la Rosa, Núñez-Gastélum, Vazquez-Flores and Gonzalez-Aguilar [6], the three-dimension structure of pancreatic α-amylase was obtained from Protein Data Bank (code 1PIF), and used as template. Ligand structures, HES, LUT, QUE, CAT, RUT and ACA, were obtained from PubChem data base (USA) and minimized using PyMOL software v. 1.3 (USA). Automated molecular docking studies of the ligand at the pancreatic α-amylase were performed with AutoDock Vina using the interphase installed in USCF-Chimera v. 4 (USA) run with the default parameters and a search volume of approximate the same size as pancreatic α-amylase. The three-dimensional structure of the enzyme was considered rigid, and the ligands structures were

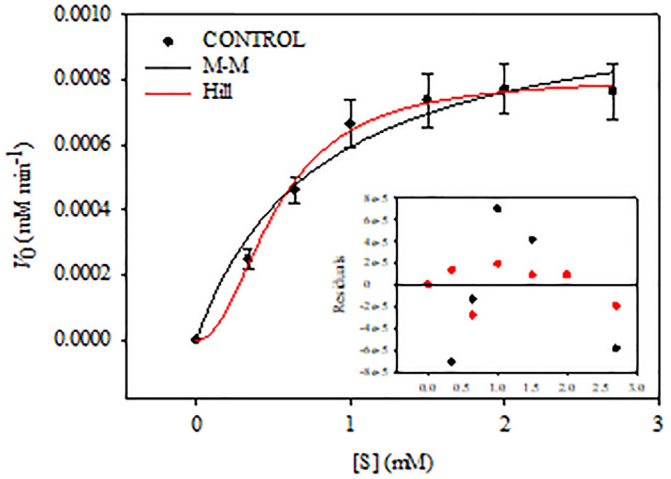

Fig. 2. Control activity of α-Amylase reaction with *p*NPG5. Symbols represent average of experimental data ± standard deviation. Black and red lines are the Michaelis-Menten (M-M) and the Hill fitted curves to the experimental data. Inset shows residuals of M-M (black) and Hill (red).

considered flexible during the performance. According to the scores and binding energy value (herein refers to Δ*G* value), the best pose for each ligand was obtained and analyzed.

Molecular Potential Surface analyses were made with the Adaptive Poisson-Boltzmann Solver [27] using the PDB 2PQR Web portal (USA). The PQR (for per-atom charge and radius) file was generated using the PARSE force field. The PROPKA program [28] was used to assign the protonation state of enzyme at pH 7.0. 100 mM of ion salt was set. The rendered electrostatic potential was visualized using the plug-in Adaptive Poisson-Boltzmann Solver of the USFC-Chimera software (USA).

2.6. Statistical Analysis of the Enzyme Kinetics and the Binding Experiments

All the experimental assays were run in triplicates. Results are expressed as mean values ± standard deviation. Analysis of variance and Fisher least significant difference analysis was performed by SPSS v. 20 software (USA) for the determination of statistically significant differences between treatments with a level of significance of 0.05.

3. Results and Discussion

3.1. Inhibition of Pancreatic α-Amylase Activity

The activity of pancreatic α-amylase was measured in absence and presence of flavonoids, HES, LUT, QUE, CAT and RUT, and the positive control ACA (Fig. 1) at different *p*NPG5 concentrations (0.3–2.7 mM). The inhibition percentage (Eq. (1)) at different concentration of compounds and a fixed substrate concentration (2.7 mM, saturation concentration) showed a hyperbolic trend (data not shown). To compare the inhibitory capacity of the analyzed compounds, the half maximal inhibitory concentration (IC_{50}) were determined. The IC_{50} values for HES, LUT, QUE and ACA were 20.10 ± 0.70, 18.00 ± 1.00, 12.70 ± 1.20, and 14.60 ± 1.70 μM, respectively. These results agree with those of Tadera, Minami and Takamatsu [15], which observed that the flavonoid LUT was the best inhibitor for the same enzyme (lower IC_{50} value), followed by other flavonoids such as QUE. They suggested that the double bond between C2 and C3 from ring C of flavonoids could be responsible for the higher inhibitory activity.

A sigmoidal behavior was observed for the substrate saturation kinetics (Fig. 2). An apparent cooperativity was determined from the calculated Hill coefficient (*h*) of 2.09 ± 0.43 (Table 1) (Eq. (3)). Fig. 2 inset represents the residuals analysis for each non-linear regression, where it is possible to observe that the adjustment with Hill coefficient showed lower residuals compared to those obtained with the classical Michaelis-Menten analysis. Hill coefficient is commonly used to estimate the quantity of ligand molecules that bind to the receptor within a functional effect in its enzymatic activity, but this coefficient is properly used to reflect cooperativity between enzyme forms or active sites [29]. In our study, this cooperativity (*h* of 2) could be explained by means of a kinetic cooperativity mechanism, were at least two forms of the enzyme are present in an equilibrium [30,31]. The binding of flavonoids to the enzyme shifts the equilibrium toward one of the enzyme forms except in the cases of LUT and QUE at their lowest concentration, were two sites were observed (no significant difference ($p < 0.05$) of *h* respect to control). This behavior of one binding site per enzyme in the presence of PC has been reported for different enzymes [32].

The α-amylase-flavonoids interactions could inactivate one of the enzyme conformational forms by displacing the equilibrium to the most stable conformational form. The effect of flavonoids and ACA on pancreatic α-amylase activity is shown in Fig. 3. HES, LUT and QUE significantly induced ($p < 0.05$) enzyme inhibition compared to control

Table 1
Pancreatic α-amylase apparent catalytic parameters (V_{max}, K_M, K_i and K_i') and Hill coefficient (*h*) values for the hydrolysis of *p*NPG5 in the presence of the flavonoids and ACA.

Ligand	Concentration (μM)	V_{max} ($\cdot 10^{-4}$ mM min^{-1})	K_M (mM)	*h*	K_i and K_i' (mM)	
CONTROL	0.00	10.65 ± 0.48^a	0.79 ± 0.03^d	2.09 ± 0.43^a	n.d.	n.d.
HES	6.30	8.69 ± 0.60^b	0.81 ± 0.00^d	1.22 ± 0.08^b	1.89 ± 0.32^b	7.50 ± 2.00^a
	12.60	7.48 ± 0.16^c	0.86 ± 0.06^d	1.03 ± 0.11^b		
	25.00	7.20 ± 0.31^c	1.04 ± 0.10^c	1.05 ± 0.20^b		
LUT	6.40	10.77 ± 0.38^a	2.11 ± 0.18^b	1.67 ± 0.38^a	1.24 ± 0.10^b	2.55 ± 0.68^b
	12.67	9.70 ± 0.42^b	2.86 ± 0.62^a	1.16 ± 0.09^b		
	25.35	7.35 ± 0.06^c	3.38 ± 0.51^a	1.03 ± 0.15^b		
QUE	12.51	10.27 ± 0.12^a	1.09 ± 0.00^c	1.72 ± 0.34^a	1.72 ± 0.50^b	3.94 ± 0.90^b
	24.83	9.51 ± 0.33^b	1.79 ± 0.16^b	1.30 ± 0.16^b		
	49.66	8.49 ± 1.00^{bc}	1.92 ± 0.02^b	1.17 ± 0.05^b		
CAT	12.32	10.51 ± 0.19^a	0.73 ± 0.03^e	1.28 ± 0.10^b	n.d.	n.d.
	24.45	10.40 ± 0.15^a	0.72 ± 0.05^e	1.21 ± 0.09^b		
RUT	12.84	11.10 ± 0.60^a	0.77 ± 0.01^e	0.96 ± 0.10^b	n.d.	n.d.
	25.57	11.07 ± 0.29^a	0.87 ± 0.02^d	0.91 ± 0.13^b		
ACA	9.00	9.99 ± 0.16^a	0.86 ± 0.14^d	0.55 ± 0.04^c	9.48 ± 1.65^a	n.d.
	17.99	10.02 ± 0.11^a	1.30 ± 0.22^c	0.52 ± 0.00^c		
	24.86	10.01 ± 0.20^a	1.73 ± 0.24^b	0.58 ± 0.07^c		

The data are presented as mean value ± standard deviation of triplicate analysis. Different letters in the same row indicate statistically significant values (Fisher's least significant difference analysis, $p \leq 0.05$) respect to control, or between treatments for K_i and K_i'. n.d. = not determined.

(Fig. 3a, b and c, respectively). LUT and QUE effects can be compared with ACA, which also had a decreasing effect over the enzymatic activity (Fig. 3f). CAT and RUT did not induce enzyme inhibition (Fig. 3d and e, respectively). Contrary to our results, Fontana Pereira, Cazarolli, Lavado, Mengatto, Figueiredo, Reis, Guedes, Pizzolatti and Silva [33] evaluated the inhibitory activity of RUT in an *in vivo* model, observing an inhibition of the enzyme, however, the possible inhibitory mechanism of RUT against pancreatic α-amylase remains unclear.

Apparent K_M and V_{max} values are reported in Table 1. HES, LUT and QUE showed significantly higher apparent K_M values, compared to control. These apparent K_M changes (increase) for HES, LUT and QUE, accompanied by decreasing apparent V_{max} indicated a mixed-type inhibition [34]. Similar results were observed for ACA. As shown in Fig. 3, CAT and RUT exhibited no differences on apparent K_M and V_{max} values respect to control. The mixed-type inhibition of PC over α-amylase activity has been reported by other authors [14,35]. Mixed inhibition modes for HES, LUT, QUE and ACA were determined also by Lineweaver-Burk plots (data not shown). Similar mixed inhibition mode for ACA has been reported for human pancreatic α-amylase [36]. Further studies are required because non-competitive [37], and

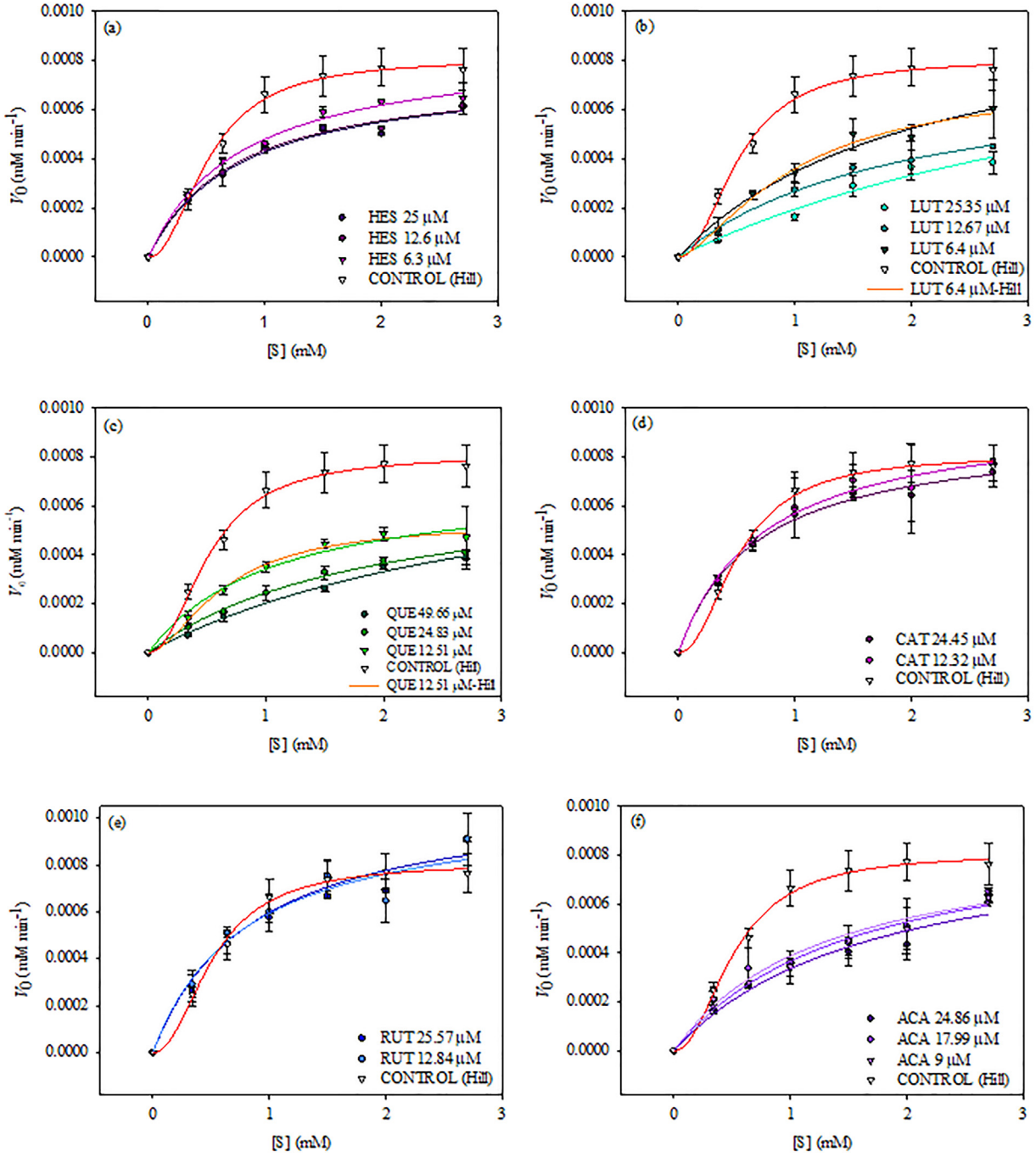

Fig. 3. Effect of HES (a), LUT (b), QUE (c), CAT (d), RUT (d), and ACA (e) on α-amylase reaction with *p*NPG5 as substrate. Different concentrations of ligands from 6.30 to 49.96 µM, were used, depending of the ligand. Symbols represent experimental data ± standard deviation. Black lines are the M-M curves fitted to the average experimental data. Red (control) and orange (LUT and QUE) lines are Hill curves fitted to the average experimental data.

competitive [5,38] modes for ACA have been reported. Probably in these studies, even though a mixed inhibition mode exists, authors have only observed one of the two components of a mixed inhibition mode.

Different phenolic acids (chlorogenic acid derivatives) exhibited this inhibition mode, which was attributed to a decrease in the substrate binding affinity toward the active site, after the inhibitor bound to this site [14]. The K_i values lower than K_i' values also support the mixed-type inhibition mechanism in which the inhibitor binds tighter to the free enzyme (competitive inhibition), than to the enzyme-substrate form [35]. HES, LUT and QUE showed no significant difference among them on K_i, which indicated that they all present the same competitive effect. The competitive inhibition constant for LUT was lower than its K_M values, supporting the idea that LUT can compete with the substrate for the binding site. Interesting, the lower K_i value for LUT compared to QUE, could be associated to the structural difference between them: the hydroxyl group at position 3, which could be responsible of the higher inhibitory effect of LUT. The relevance of C-ring planarity (3-hydroxyl group lacking and C2═C3 double bond) has been reported in the inhibition of other enzymes, such as vascular endothelial grow factor [39]. Throughout SAR analysis, the lack of α-amylase inhibitory activity of CAT may be explained considering the flexibility of this molecules due to the presence of saturated C2—C3 bond which allows B-ring to twist [39] preventing it to fit into its binding site. Similar results using SAR analysis for multidrug resistance-associated protein 1 (MRP1) inhibition by flavonoids showed that dihedral angle on saturated C2—C3 negatively affected the inhibition [40].

3.2. Binding of Flavonoids to Pancreatic α-Amylase by Fluorescence Spectroscopy

The observed change in the intrinsic fluorescence from pancreatic α-amylase (absence and presence of ligands) can be associated mainly to the 19 Trp residues of the enzyme [12]. Trp residues present relatively high absorbance in comparison to Tyr, and the decrease in the intrinsic fluorescence has been associated to an increase in the polarity of Trp surroundings [41]. Fig. 4 shows the FI values for each ligand after inner-filter effect correction. The highest FI observed were for LUT and QUE, followed by HES and RUT. A non-linear regression analysis was carried out with a calculated ΔFI_c to obtain the K_D value (Eq. (7)) for each ligand (Table 2), except for CAT, which did not exhibit any changes in fluorescence. The higher ΔFI observed for LUT and QUE could be related to their structures. Both compounds present two structural characteristics that seemed to be relevant for quenching process: (i) the catechol moiety and (ii) the C2═C3 double bond in B-ring. When

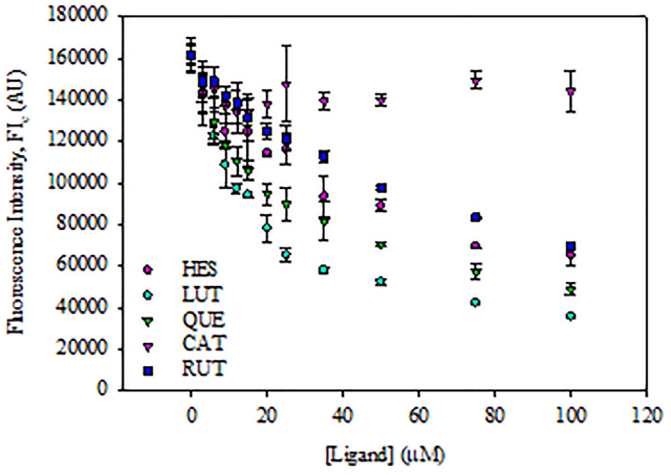

Fig. 4. Effect of the flavonoids HES, LUT, QUE, CAT and RUT (ligands) on α-amylase intrinsic fluorescence intensity. Different concentrations (3–100 μM) of the ligands were tested, and the fluorescence intensity was corrected for inner effects (IF_c). Symbols represent the average of three experimental data replicates.

analyzing the redox ability of these compounds it has been reported that beside these two characteristics, the carbonyl group at C-4 seems to be relevant in their activity [42]. The catechol moiety of the B ring seems to be important in the interactions between flavonoids and proteins, such as MRP1 transporter [40]. Similar effects have been observed between pancreatic α-amylase and chlorogenic acid derivatives [14]. This dihydroxyl group (catechol) in ring C has been noticed as a requirement for antioxidant activity of flavonoids [16]. In contrast to flavonoids, ACA didn't show any effect on the intrinsic fluorescence of pancreatic α-amylase, in agreement with previous results [43]. This may be explained considering that ACA did not modify the Trp environment on enzyme, especially of Trp^{58} and Trp^{59} that are located near the active site.

Fig. 5a–d presents the Stern-Volmer plots for HES, LUT, QUE and RUT, respectively. The linearity on the fitting of the experimental values to Eq. (9) assures that a single quenching mechanism is occurring. From the calculated k_q values, it is possible to propose that the four flavonoids followed a static mechanism [23]. Static quenching is characterized by the formation of a ground-state complex between quencher and fluorophore. This mechanism has been observed between pancreatic α-amylase and PC extracts such as procyanidins [12,44]. K_A and n values, calculated using Eq. (9) are also presented in Table 2. The n values, which were approximately 1, referred that each flavonoid presents one binding site with the enzyme, in agreement with the kinetic results (Hill coefficient, Table 1), indicating that there is only one binding site per enzyme molecule. In this way, the presence of the flavonoid would benefit one conformational form of the enzyme (hill coefficient, $h \sim 1$), in which the binding site would be occupied by them ($n \sim 1$) as part of the estimated reversible mixed-type inhibition mechanism.

It seems that a higher quenching result corresponded to a higher inhibitory activity of flavonoids. Fig. 5b and Table 2 show that a lower K_A was observed for the flavonoid (LUT) with a high K_i value for the interaction with α-amylase. Similar results have been reported for green tea polyphenolic extract [45,46]. LUT seemed to be the quencher with the highest binding affinity for the protein (lowest K_A), and a lower dissociation rate for the protein-LUT complex than the other flavonoids (higher K_i value). RUT also presented a higher K_A, but it seemed that the binding of this ligand on protein has no significant effect over its enzymatic activity. Higher K_A values and lower inhibition of pancreatic lipase activity for RUT than other PC were observed [47]. These could be explained considering that the RUT sugar moiety could be interacting with the subsites −1 to +1 on the enzyme active site, acting as a substrate analog.

K_{sv} and k_q values were calculated with Eq. (8), and results are shown in Table 2. In agreement with the structural features of LUT and QUE discussed above in the kinetics section, LUT and QUE presented the highest K_{sv} and k_q values, followed by HES, RUT, and CAT. Higher K_{sv} value corresponds to more thermodynamically spontaneous enzyme-ligand reactions, and a stronger affinity [44,48]. Table 2 shows that the calculated K_{sv} and k_q for LUT corresponded to the best quencher [5,49]. This higher affinity of LUT may be explained considering the C-ring planarity, which increased the opportunity to interact with the enzyme. k_q values higher than the maximal dynamic quenching constant ($1.0 \cdot 10^{10}\ M^{-1}\ s^{-1}$) [23] indicates that the quenching occurred mainly through the formation of a ground state complex between the fluorophore (enzyme) and the quencher (flavonoid). This quenching mechanism is referred as static, and it has been reported for α-amylase-PC interactions, such as in the interactions of this enzyme with procyanidins [22,44].

3.3. Interaction Between Pancreatic α-Amylase and Flavonoid by Extrinsic Fluorescence

Changes in extrinsic fluorescence of ANS were performed to deeply understand the binding mechanism of the tested flavonoids over α-amylase. ANS produced an uncompetitive inhibition of enzyme activity

Table 2
Quenching parameters ($_{app}K_D$, K_{sv}, k_q, n and K_A) of pancreatic α-amylase fluorescence for the flavonoids, HES, LUT, QUE, CAT and RUT.

Ligand	$_{app}K_D$ (μM)	K_{sv} ($\cdot 10^{-1}$ mM^{-1})	k_q ($\cdot 10^{-12}$ mM^{-1} s^{-1})	n	K_A ($\cdot 10^{-1}$ mM^{-1})
HES	47.45	1.18 ± 0.46^{b}	4.00 ± 1.03^{b}	1.17 ± 0.08^{a}	1.68 ± 0.05^{b}
LUT	21.01	3.18 ± 0.62^{a}	10.71 ± 2.10^{a}	1.09 ± 0.11^{a}	5.30 ± 0.41^{a}
QUE	19.92	2.19 ± 0.47^{a}	7.38 ± 1.70^{a}	0.82 ± 0.17^{a}	1.64 ± 0.09^{b}
CAT	n.d.	0.00 ± 0.00^{c}	0.00 ± 0.00^{c}	0.59 ± 0.17^{ab}	0.00 ± 0.00^{c}
RUT	61.47	1.14 ± 0.11^{b}	3.84 ± 0.55^{b}	1.53 ± 0.29^{a}	4.50 ± 0.20^{a}

The data are presented as mean value ± standard deviation of triplicate analysis. Different letters in the same row indicate statistically significant values (Fisher's least significant difference analysis, $p \leq 0.05$) between treatments. n.d. = not determined.

(data not shown). However, ANS exhibited an IC_{50} value higher (>150 μM) than LUT, QUE and ACA (<20 μM).

The fluorescence intensity of ANS complexed with the enzyme was measured. In presence of the ligands LUT, QUE, RUT and ACA the intensity decreased in a dose-dependent manner (Fig. 6b–c, and e–f, respectively). Docking analysis suggested that ANS binds near the active site and flavonoids binding site (data not shown). Consequently, the decrease in fluorescence intensity could be explain considering that ANS and flavonoids, LUT, QUE and RUT, may be competing for the same binding site. HES exhibited an increase in the ANS fluorescence, and CAT did not produce any significant change in the fluorescence intensity (Fig. 6a and d, respectively). A double bond between C2 and C3 of flavonoids, which is not present in HES and CAT, has been associated with a more rigid structure of the flavonoids [39]. In agreement with the results obtained by fluorescence quenching and enzyme activity, the lack of this double bond could decrease the interaction of these molecules with α–amylase, resulting in a lower displacement of ANS in the ANS-enzyme-flavonoid ternary complex. However, further studies are required since similar inhibitory activities were observed for LUT, QUE and HES, despite this C2═C3 double bond, which is not present in HES.

The maximum emission peak for ANS-α-amylase complex was at 519 nm. This maximum changed for some flavonoids. A bathochromic (blue) shift was observed for LUT (9 nm) and RUT (14 nm), respectively (Fig. 6b and e). This shift was attributed to a reduction in the mobility of ANS in the binding site [50], suggesting that its binding site in the protein has been blocked due the structural change produced by the flavonoids interactions with the binding site, which make it unavailable for the ANS. Whereas a hypsochromic (red) shift (Fig. 6c) was observed for QUE (over 9 nm), which suggested an increase in solvent polarity and an exposure of the binding hydrophobic residues such as Trp [51]. Fluorescence (quenching and ANS) results suggested that the protein-flavonoid interaction probably induce a conformational change near the binding site that mainly affects the Trp residues of this region (like 58 and 59).

The ANS fluorescence change is used as an indirect assay to measure the binding of ligands to enzymes. Apparent K_D ($_{app}K_D$) values were

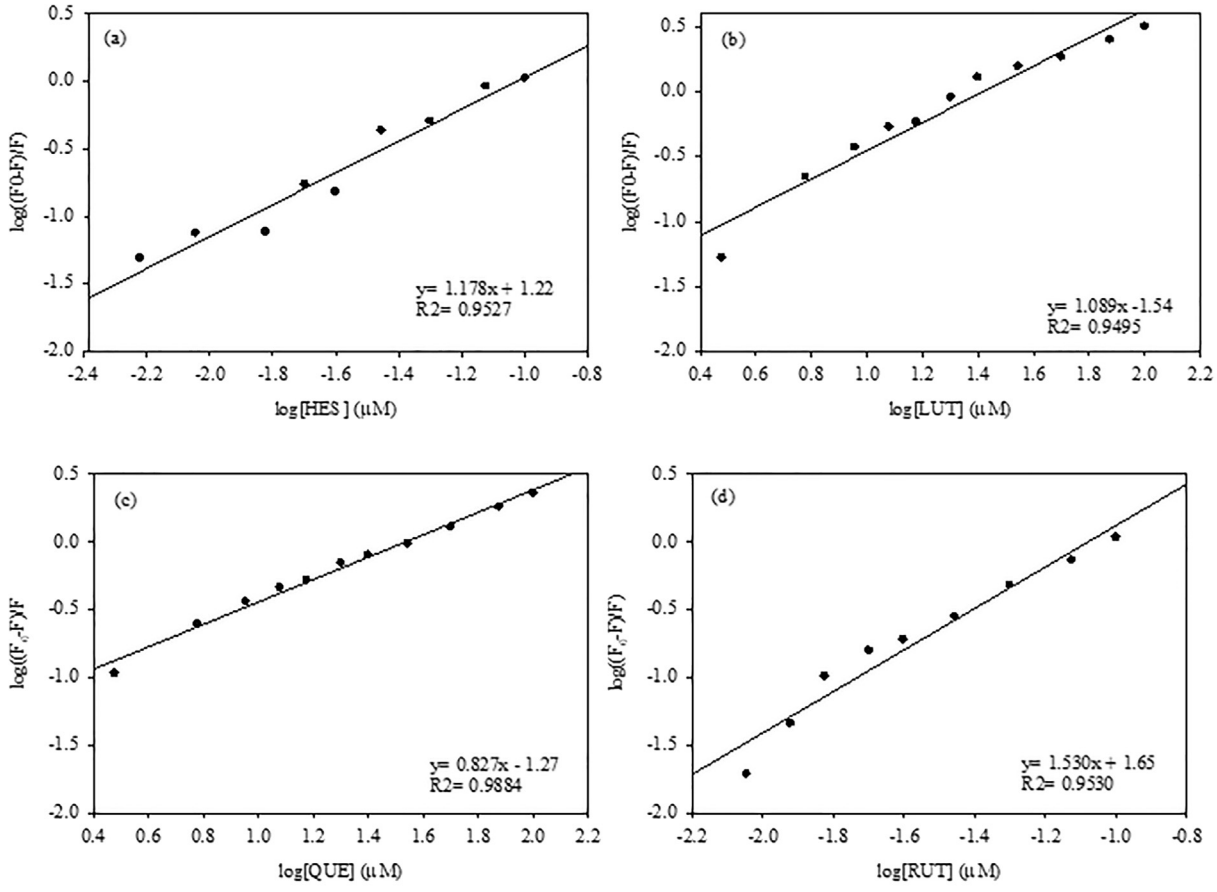

Fig. 5. Quenching effect of flavonoids on α-amylase fluorescence intensity. Plot of log(($F_0 - F$) / F) against log[quencher] were elaborated for the ligands HES (a), LUT (b), QUE (c), and RUT (d). The lines correspond to the linear curve fitting done for the experimental data.

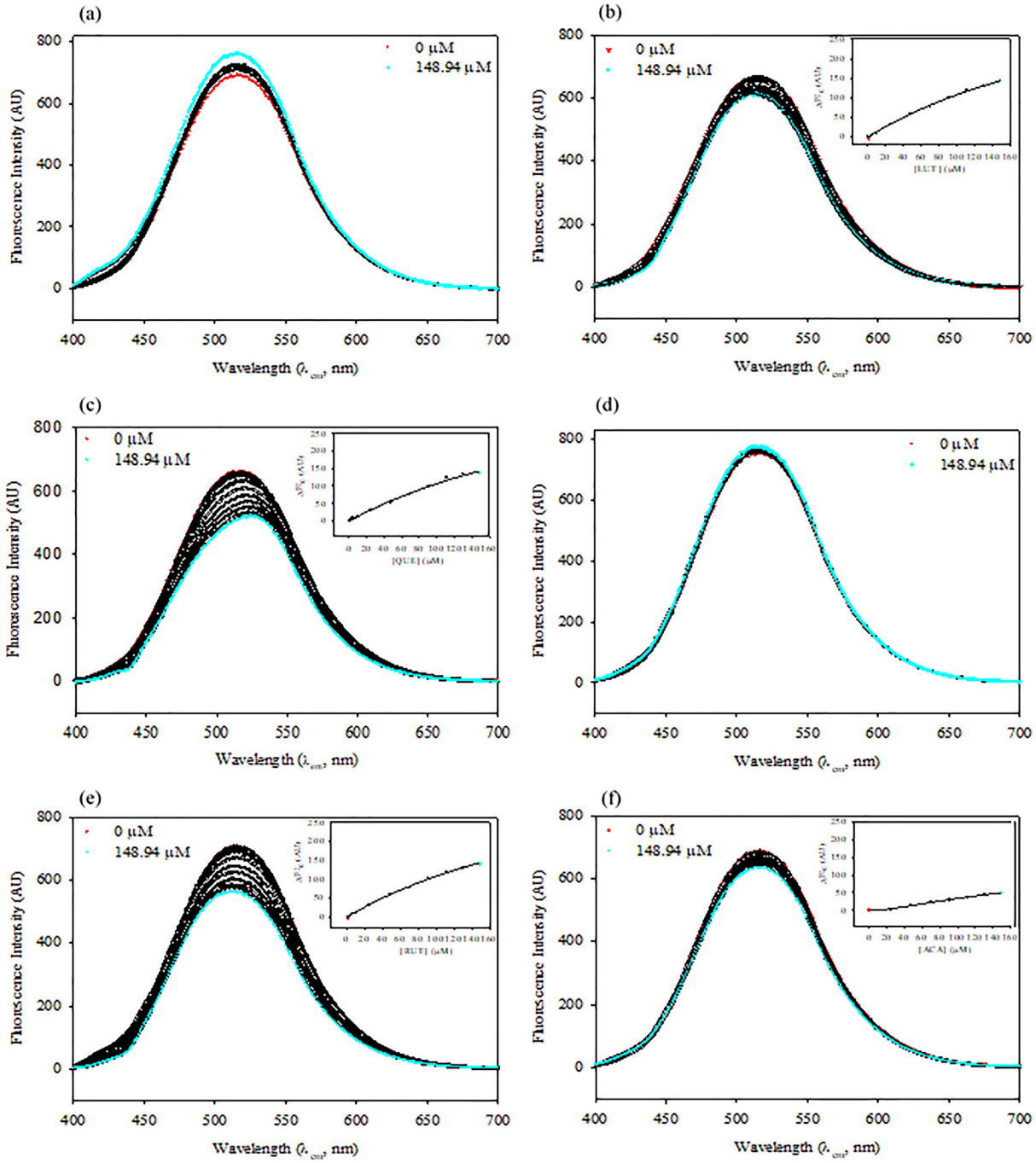

Fig. 6. Fluorescence spectra of pancreatic α-amylase-ANS complex in the absence and presence of different concentrations (1–148.94 μM) of ligands: HES (a), LUT (b), QUE (c), CAT (d), RUT (e) and ACA (f). Inset shows plot ligand concentrations (μM) *versus* corrected fluorescence intensity change (ΔFI_c, AU).

calculated from non-linear curve fittings of ΔFI_c *versus* ligand concentration (inset plots on Fig. 6b, c, e and f). These values were associated to the affinity of enzyme-ligand complex, because it corresponds to ANS displacement from the enzyme surface by the flavonoid. LUT, QUE, RUT and ACA exhibited $_{app}K_D$ values of 207 ± 19.5, 350 ± 24.0, 315 ± 14.0, and 150 ± 18.1 μM, respectively. The ANS had lower affinity

Table 3
The energy results (kCal mol^{-1}), the amino acids residues lining the binding site in α-amylase cavity, and the distance (Å) for the possible enzyme-ligands conformations.

Ligands	Amino acid residues lining the binding site, distance and binding energy			
	Interaction van der Waals forces	Hydrophobic binding	Hydrogen binding	ΔG
HES	None	Trp^{58} (3.7), Trp^{59} (3.7; 3.7), Tyr^{62} (3.8)	Gln^{63} (2.8), Asp^{197} (2.9)	−8.7 (Site 2, S2)
LUT	Leu^{165} (3.4)	Trp^{58} (3.6), Trp^{59} (3.7)	Trp^{59} (3.6), Gln^{63} (2.8), Arg^{195} (3.3), Asp^{197} (2.7)	−9.0 (S2)
QUE	Leu^{165} (3.3), Trp^{59} (3.7)	Trp^{59} (3.5; 3.7)	Gln^{63} (3.3), Arg^{195} (3.3), Asp^{197} (2.7)	−8.7 (S2)
CAT	None	Trp^{58} (3.8), Trp^{59} (3.6; 3.6), Tyr^{62} (3.9)	Gln^{63} (3.0; 3.2), Arg^{195} (3.4), Asp^{197} (3.2)	−8.4 (S2)
RUT	Val^{163} (3.7)	Trp^{58} (4.1), Tyr^{62} (3.9)	Gln^{63} (2.8), Asp^{197} (3.1; 3.1), Arg^{195} (3.2), Asp^{300} (2.4)	−8.5 (S2)
ACA	None	Phe^{335} (3.7; 3.8), Asp^{402} (4.0)	Gln^{5} (3.7), Thr^{6} (2.9; 3.1), Arg^{398} (2.8; 3.2), Gly^{403} (3.6)	−8.2 (S3)

(higher $_{app}K_D$ values) for the enzyme in presence of the flavonoids like QUE and LUT, which indicates stronger bindings between enzyme and flavonoid complex compared to the enzyme-ANS complex, in presence of these flavonoids. These results agreed with their lower $_{app}K_D$ values calculated from quenching.

The enzyme-ANS in presence of ACA showed the strongest binding affinity (lower $_{app}K_D$ value), but it cannot be compared because an $_{app}K_D$ value was not calculated by the intrinsic fluorescence assay. No changes on the intrinsic fluorescence assay were observed. It is suggested that ACA interaction produced a conformational change on enzyme. In consequence Trp^{58} and Trp^{59} were covered, and no changes in intrinsic fluorescence were observed. This behavior could be explained considering that the conformational changes produced by ACA confer stability to the enzyme-ANS complex. Enzyme-ANS binding was probably stronger (lower $_{app}K_D$) in presence of ACA than with flavonoids, because the enzyme-ACA interaction avoided the exposure of these two Trp residues located near to the active site on the enzyme. These two residues are essential for α-amylase catalytic activity [52],

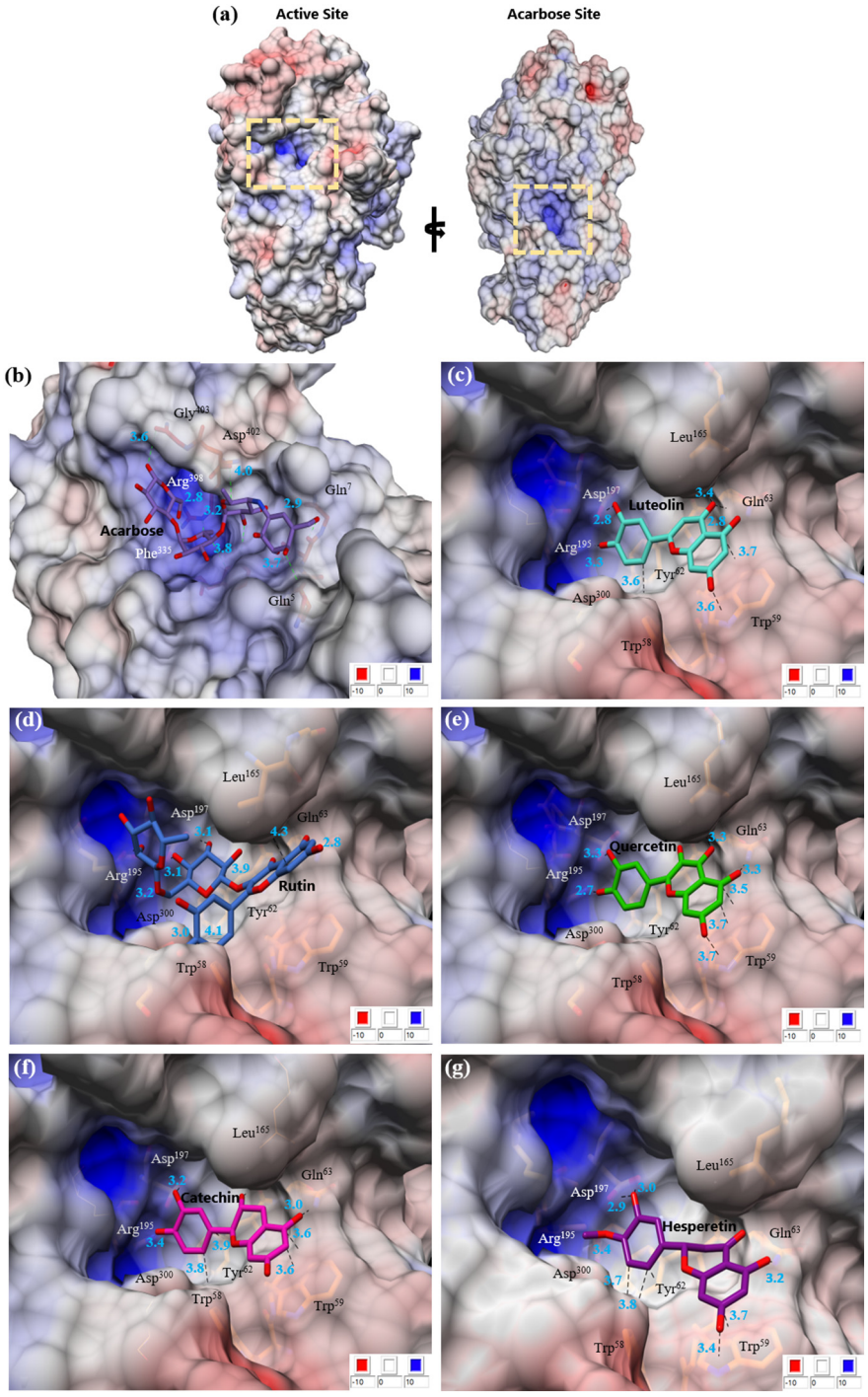

Fig. 7. Surface electrostatic potentials of the molecular surface of α-amylase polyphenol binding sites and acarbose. (a) Side view of the binding sites of the enzyme molecule; (b) acarbose binding site; (c) luteolin; (d) rutin; (e) quercetin; (f) catechin; (g) hesperetin binding sites. The color depicted over surface are −10 kT/e red, and 10 kT/e blue. Potential amino acid residues involved in binding and ligands are shown as sticks. Distance of potential interactions between enzyme and ligands are given in Å and are depicted as dashed lines. These images were generated using USFC-Chimera, and the potential map calculated using APBS-pdb2pqr (USA) at pH of 7.0 and 100 mM of salt.

then the observed inhibitory effect for ACA on enzymatic activity can be associated to the covering of these two residues. In this way, further studies are required.

3.4. Molecular Docking

The analysis of possible binding sites for flavonoids and ACA on pancreatic α-amylase was carried on *in silico* by docking studies (Table 3). Two binding sites were predicted, one where all flavonoids bind and another for the binding of ACA. The location of flavonoids binding site was close to enzyme active site, Asp^{197}, Glu^{233} and Asp^{300}. Docking of the substrate (*p*NPG5) indicated the proximity of flavonoids binding site to the catalytic site (data not shown). Pancreatic α-amylase possesses seven subsites along the v-shaped cavity, which contains the catalytic site inside the main domain ("A" domain) of the enzyme, titled from −4 to +3 [53,54]. Starch, a natural substrate of enzyme, and *p*NPG5 may bind to the catalytic residues in the complex-model. The two different binding sites predicted for flavonoids and acarbose sites, agreed with the different kinetic and fluorescence results observed among these ligands.

Table 3 shows the predicted interactions between amino acid residues with flavonoids. The binding predictions for flavonoids were associated to hydrogen bindings, consistently with other studies of α-amylase-polyphenolic interactions [55] or even for complexes with other enzymes, such as lipase [6]. Hydrogen binding, hydrophobic binding and Van der Waals forces were the main interactions between α-amylase and PC [5]. Flavonoids may bind to a site on α-amylase composed mainly by five amino acid residues: Trp^{58}, Trp^{59}, Tyr^{62}, Gln^{63} and Asp^{197}. In agreement with the quenching studies, it can be proposed that the enzyme-LUT complex was stabilized through two bindings types (hydrogen and hydrophobic) with Trp^{59}, and one hydrogen binding interaction of 2.1 Å with Gln^{63}. QUE showed hydrogen binding with Gln^{63} (2.2 Å), and Van der Waals forces with Leu^{165}. These results could explain the higher inhibitory capacities of LUT and QUE, where the complexes formed by a static quenching mechanism, would be stabilized trough hydrogen bindings between hydroxyl groups of catechol (B-ring) and atoms such as amino from the protein.

The enzyme-RUT complex included different amino acids such as Val^{163}, Glu^{233} and Asp^{300}. Asp^{300}-RUT interaction maybe related to a higher affinity for the flavonoid. In another study, docking results between a glycosylated flavonoid (resveratrol-3-O-glucoside) with this residue of α-amylase chain were also reported [12]. They concluded that an interaction with this residue did not ensure an inhibitory effect on the enzymatic catalysis, since its function remains unclear. The prediction for the complex with ACA showed that this molecule interacted with amino acid residues Gln^{5}, Thr^{6}, Thr^{11}, Pro^{332}, Gly^{334} and Phe^{335}, which are located in the opposite region of the enzyme respect to the active site. These results agree with fluorescence results, in which no complex formation between enzyme and ACA was observed, and with the lack of displacement of ANS fluorescence intensity, which may indicate that ACA binds with the enzyme in a different binding site.

The difference in the inhibition modes between flavonoids and ACA may be associated with these different binding sites. The inhibition of the enzymatic activity by ACA could be explained by the proximity of this compound to the catalytic residues. From this point, ACA avoid the interaction of substrate with its binding site, by covering two amino acids participating in the substrate union, Trp^{58} and Trp^{59}. Nevertheless, further studies are required about the inhibitory mechanism of ACA on pancreatic α-amylase. Authors such as Al-Asri, Fazekas, Lehoczki, Perdih, Görick, Melzig, Gyémánt, Wolber and Mortier [10] pointed it out as a competitive inhibitor with a binding site near to enzyme active site, according to docking. Contrarily, other authors such as [Li, Begum, Numao, Park, Withers and Brayer [38]] designated ACA as a mixed-type inhibitor (non-competitive), ACA and its analogues like isoacarbose could bind to human pancreatic α-amylase on a different subsite (+3).

In order to better explain these results, Molecular Potential Surface analyses were carried out. Fig. 7 is the result of the Molecular Docking and Molecular Potential Surface analyses. The results for the docking analysis were described above (Table 3). Molecular Potential Surface analysis results presented in Fig. 7 are related to the electrostatic potential of the enzyme and the ligand to interact between them. The two possible binding sites described, one for flavonoids and another for ACA are shown in Fig. 7a. Red and blue colors on protein surface represented the negative and positive electrostatic distributions, respectively. This figure shows that the binding site for ACA (Fig. 7b) was in a positive area on protein, where the oxygen atoms from carbonyl groups in ACA presented the main interactions. In the case of flavonoids, a low negative potential observed between the aromatic residues of the enzyme and the rings present in the flavonoids may indicate the formation of some *pi*-stacking type interactions, instead of London dispersion interactions. In all cases, in agreement with docking analysis, hydroxyl groups of B ring appear to participate in a H-bond from the positive region of the active site (A and G1 subsites, [56]). C and A rings bind to subsites A and G. Fig. 7d shows that, the sugar moiety of rutin occupies the sugar binding sites −1 and 1 of the active site, in agreement with docking and fluorescence results.

4. Conclusion

HES, LUT and QUE exhibited inhibitory capacity against α-amylase activity, by hydrogen and hydrophobic bindings. This effect was explained by the higher affinity between these flavonoids with the enzyme as observed by fluorescence spectroscopy. ANS results showed that the binding of flavonoids (same binding site for flavonoids and ANS) correspond to a hydrophobic interaction. It seems that even though CAT and RUT maybe able to bind with enzyme, they did not have a significant inhibitory effect on the enzymatic activity. The observed LUT inhibitory effect was higher than the ACA, which can be attributed to the different binding site of ACA. The flavonoids modified the apparent kinetic cooperativity of pancreatic α-amylase (observed in their absence), and one binding site on the protein would exist for them. The SAR analysis allowed pointing out three characteristics from LUT structure that facilitates its α-amylase inhibition: double bond between C2 and C3 (ring A); catechol structure for B ring; and planarity of C ring, which is the only difference from QUE structure.

Acknowledgements

The authors are grateful for the financial support from CONACYT, Mexico (CB-2016-01-286449). A.I.M.G. is grateful for the PhD scholarships from CONACYT and the support from UACJ.

References

[1] R. Guha, Methods Mol. Biol. 993 (2013) 81–94.
[2] E. Bendary, R.R. Francis, H.M.G. Ali, M.I. Sarwat, S. El Hady, Ann. Agric. Sci. 58 (2013) 173–181.
[3] A. Muhammad, Ind. Crop. Prod. 78 (2015) 66–72.
[4] T. Buchholz, M.F. Melzig, Planta Med. 81 (2015) 771–783.
[5] A.I. Martinez-Gonzalez, Á.G. Díaz-Sánchez, L.A. d.l. Rosa, C.L. Vargas-Requena, I. Bustos-Jaimes, E. Alvarez-Parrilla, Molecules 22 (2017) 669.
[6] A.I. Martinez-Gonzalez, E. Alvarez-Parrilla, Á.G. Díaz-Sánchez, L.A. de la Rosa, J.A. Núñez-Gastélum, A.A. Vazquez-Flores, G. Gonzalez-Aguilar, Food Technol. Biotechnol. 55 (2017) 519–530.
[7] Y. Tan, S.K.C. Chang, Y. Zhang, Food Chem. 214 (2017) 259–268.
[8] P. Hemalatha, D. Bomzan, B.V. Rao, Y.N. Sreerama, Food Chem. 199 (2016) 330–338.
[9] X. Yang, F. Kong, LWT Food Sci. Technol. 66 (2016) 232–238.
[10] J. Al-Asri, E. Fazekas, G. Lehoczki, A. Perdih, C. Görick, M. Melzig, G. Gyémánt, G. Wolber, J. Mortier, Bioorg. Med. Chem. 23 (2015) 6725–6732.
[11] M. Bhandari, N. Jong-Anurakkun, G. Hong, J. Kawabata, Food Chem. 106 (2008) 247–252.
[12] M. Miao, H. Jiang, B. Jiang, T. Zhang, S. Cui, W.Z. Jin, Food Chem. 145 (2014) 205–211.
[13] K. Sakulnarmrat, G. Srzednicki, I. Konczak, LWT Food Sci. Technol. 57 (2014) 366–375.
[14] Y. Narita, K. Inouye, Food Chem. 127 (2011) 1532–1539.
[15] K. Tadera, Y. Minami, K. Takamatsu, J. Nutr. Sci. Vitaminol. 52 (2006) 149–153.

[16] J. Xiao, X. Ni, G. Kai, X. Chen, Crit. Rev. Food Sci. Nutr. 53 (2013) 497–506.
[17] R. Gonçalves, N. Mateus, D.V. Freitas, Food Chem. 125 (2011) 665–672.
[18] A. Dalar, I. Konczak, Ind. Crop. Prod. 44 (2013) 383–390.
[19] V.V. Heredia, J. Thomson, D. Nettleton, S. Sun, Biochemist 45 (2006) 7553–7562.
[20] K.F. Tipton, Patterns of enzyme inhibition, in: P.C. Engel (Ed.), Enzymology Labfax, BIOS Scientific Publishers, Oxford 1996, pp. 115–171.
[21] A.G. Diaz-Sanchez, E. Alvarez-Parrilla, A. Martinez-Martinez, L. Aguirre-Reyes, J.A. Orozpe-Olvera, M.A. Ramos-Soto, J.A. Nunez-Gastelum, B. Alvarado-Tenorio, L.A. de la Rosa, Molecules 21 (2016) 1628.
[22] R. Gonçalves, N. Mateus, V. de Freitas, Food Chem. 125 (2011) 665–672.
[23] J.R. Lakowicz, Quenching of fluorescence, Principles of Fluorescence Spectroscopy, Kluwer Academic/Plenum Publishers, New York 1999, pp. 237–265.
[24] F.G. Prendergast, J. Lu, P.J. Callahan, J. Biol. Chem. 258 (1983) 4075–4078.
[25] V.M. da Silva, J.A.P. Sato, J.N. Araujo, F.M. Squina, J.R.C. Muniz, K.A. Riske, W. Garcia, PLoS One 12 (2017).
[26] H. Sun, D. Wang, X. Song, Y. Zhang, W. Ding, X. Peng, X. Zhang, Y. Li, Y. Ma, R. Wang, P. Yu, J. Agric. Food Chem. 65 (2017) 1574–1581.
[27] N.A. Baker, D. Sept, S. Joseph, M.J. Holst, J.A. McCammon, PNAS 98 (2001) 10037–10041.
[28] C.R. Søndergaard, M.H.M. Olsson, M. Rostkowski, J.H. Jensen, J. Chem. Theory Comput. 7 (2011) 2284–2295.
[29] J.N. Weiss, FASEB J. 11 (1997) 835–841.
[30] S. Darnis, N. Juge, X.J. Guo, G. Marchis-Mouren, Biochim. Biophys. Acta (1999) 281–289.
[31] G. Ferey-Roux, J. Perrier, E. Forest, G. Marchis-Mouren, A. Puigserver, M. Santimone, Biochim. Biophys. Acta 1388 (1998) 10–20.
[32] N. Kuhnert, F. Dairpoosh, R. Jaiswal, M. Matei, S. Deshpande, A. Golon, H. Nour, H. Karaköse, N. Hourani, J. Chem. Biol. 4 (2011) 109–116.
[33] D. Fontana Pereira, L.H. Cazarolli, C. Lavado, V. Mengatto, M.S. Figueiredo, B. Reis, A. Guedes, M.G. Pizzolatti, F.R. Silva, Nutrition 27 (2011) 1161–1167.
[34] P.C. Engel, Enzyme kinetics, in: P.C. Engel (Ed.), Enzymology LabFax, BIOS Scientific San Diego 1996, pp. 77–112.
[35] S. da Silva, E. Koehnlein, A. Bracht, R. Castoldi, G. de Morais, M. Baesso, R. Peralta, C. de Souza, A. de Sá-Nakanishi, R. Peralta, Food Res. Int. 56 (2014) 1–8.
[36] X. Qin, L. Ren, X. Yang, F. Bai, L. Wang, P. Geng, J. Struct. Biol. 174 (2011) 196–202.
[37] L. Dolečková-Marešová, M. Pavlík, M. Horn, M. Mareš, Chem. Biol. 12 (2005) 1349–1357.
[38] C. Li, A. Begum, S. Numao, K.H. Park, S.G. Withers, G.D. Brayer, Biochemistry 44 (2005) 3347–3357.
[39] A.B. Cerezo, M.S. Winterbone, C.W.A. Moyle, P.W. Needs, P.A. Kroon, Mol. Nutr. Food Res. 59 (2015) 2119–2131.
[40] G. Gonzales, G. Smagghe, C. Grootaert, M. Zotti, K. Raes, J. Camp, Drug Metab. Rev. 47 (2015) 175–190.
[41] F. Khan, A. Ahmad, M.I. Khan, IUBMB Life 59 (2007) 34–43.
[42] K. Brudzynski, L. Maldonado-Alvarez, Pol. J. Food Nutr. Sci. 65 (2015) 71–80.
[43] T. Yamamoto, Enzyme Chemistry and Molecular Biology of Amylases and Related Enzymes, 1994.
[44] X. Cai, J. Yu, L. Xu, R. Liu, J. Yang, Food Chem. 174 (2015) 291–298.
[45] L. Sun, M.J. Gidley, F.J. Warren, Mol. Nutr. Food Res. 61 (2017).
[46] L. Sun, F.J. Warren, G. Netzel, M. Gidley, J. Funct. Foods 26 (2016).
[47] Y.-Q. Li, P. Yang, G. Fei, Z.-W. Zhang, B. Wu, Eur. Food Res. Technol. 233 (2011) 63–69.
[48] J. Zhang, J.-H.H. Cui, T. Yin, L. Sun, G. Li, Food Chem. 141 (2013) 2229–2237.
[49] M. Skrt, E. Benedik, C. Podlipnik, N.P. Ulrih, Food Chem. 135 (2012) 2418–2424.
[50] O.K. Gasymov, B.J. Glasgow, Biochim. Biophys. Acta 1774 (2007) 403–411.
[51] A.A.A. Halim, M.S. Zaroog, H.A. Kadir, S. Tayyab, J. Saudi Chem. Soc. 21 (2017) S349–S358.
[52] N. Ramasubbu, C. Ragunath, P.J. Mishra, L.M. Thomas, G. Gyémánt, L. Kandra, Eur. J. Biochem. 271 (2004) 2517–2529.
[53] G.D. Brayer, G. Sidhu, R. Maurus, E.H. Rydberg, C. Braun, Y. Wang, N.T. Nguyen, C.M. Overall, S.G. Withers, Biochemistry 39 (2000) 4778–4791.
[54] M.A. Kazaz, V. Desseaux, G. Marchis-Mouren, E. Prodanov, M. Santimone, Eur. J. Biochem. 252 (1998) 100–107.
[55] Q. He, Y. Lv, K. Yao, Food Chem. 101 (2006) 1178–1182.
[56] M. Qian, R. Haser, G. Buisson, E. Duee, F. Payan, Biochemistry 33 (1994) 6284–6294.